Molecular simulation of *hydrophobin* adsorption at an oil-water interface

David L. Cheung*

Department of Chemistry and Centre for Scientific Computing, University of Warwick, Coventry, CV4 7AL, UK

E-mail: david.cheung@warwick.ac.uk

Abstract

Hydrophobins are small, amphiphilic proteins expressed by strains of filamentous fungi. They fulfil a number of biological functions, often related to adsorption at hydrophobic interfaces, and have been investigated for a number of applications in materials science and biotechnology. In order to understand the biological function and applications of these proteins a microscopic picture of the adsorption of these proteins at interfaces is needed. Using molecular dynamics simulations with a chemically detailed coarse-grained potential the behaviour of typical hydrophobins at the water-octane interface is studied. Calculation of the interfacial adsorption strengths indicates that the adsorption is essentially irreversible, with adsorption strengths of the order of 100 $k_{\mathrm{B}}T$ (comparable to values determined for synthetic nanoparticles but significantly larger than small molecule surfactants and biomolecules). The protein structure at the interface is unchanged at the interface, which is consistent with the biological function of these proteins. Comparison of native proteins with pseudoproteins that consist of uniform particles shows that the surface structure of these proteins has a large effect on the interfacial adsorption strengths, as does the flexibility of the protein.

*To whom correspondence should be addressed

Introduction

The adsorption of biomolecules, such as proteins, onto liquid interfaces is important in a wide variety of biological processes.[1] Formation of highly ordered protein layers on the air-water interface is the initial step in the formation of biofilms or other structures.[2] Many enzymes, such as lipases[3] that digest fats, operate in interfacial environments. Lung surfactant proteins adhere to air-water interface in pulmonary fluids, assisting in respiration and immune response.[4] Technological applications of biomacromolecules often exploit their interfacial behaviour, with common uses including foam and emulsion stabilizers,[5] biocompatible surface coatings,[6,7] and delivery of bioactives,[8] that make use of the interfacial properties of these molecules.

One increasingly interesting class of proteins, both for their biological function and technological applications, are *hydrophobins*.[9] These are small (typically 7-15 kDa) proteins, expressed by filamentous fungi, such as the *Aspergillus* genus. Hydrophobins have been traditionally divided into two classes (class-I and class-II)[10] based on their solubility and hydropathy patterns. They form a diverse range of proteins, but have a conserved pattern of disulphide bonds. Many examples also possess a distinctive surface structure, with a patch of hydrophobic residues on one face (typically covering $\sim$20% of their surface). This amphiphilic structure makes them highly surface active, which is central to many of their biological function. They play a role in the formation of sprouting bodies[11] and also mediate adhesion of fungi onto hydrophobic surfaces.[12] Understanding the molecular mechanisms that underlie the interfacial adsorption of hydrophobins may be used to further understand the biological role of these proteins and potentially allow the development of coatings to inhibit or promote fungal growth.

More recently hydrophobins have also been investigated for a number of technological applications, most of which exploit the ability of hydrophobins to adhere strongly to hydrophobic interfaces. These include the use of hydrophobins as foam[13] and emulsion stabilizers,[14] with applications in food technology. It has been demonstrated that adsorption of hydrophobins onto solid surfaces may be used to change the character (hydrophobic/hydrophilic) of the surface[15] and that they may be used to form biocompatible surfaces for biosensors.[16] The adhesion of hy-

drophobins onto the outside of drug particles to form a biocompatible coating has been recently demonstrated,[17] while attachment of hydrophobins to graphene sheets has also been used in the preparation of biomimetic composite materials.[18] Further exploitation of hydrophobins for these and other applications relies on a detailed understanding of their behaviour on a microscopic level, in particular in understanding the effects that control interfacial absorption strength and rates.

Due to this interest there have been a number of experimental studies on the behaviour of hydrophobins at liquid interfaces. Much of this has addressed the self-assembly of hydrophobins at interfaces and the structure and properties of these aggregates. Among the most commonly studied examples there are distinct differences in the structures formed at interfaces; in particular class-I hydrophobins absorb more slowly on interfaces and form distinctive fibril-like structures (rodlets),[19] while class-II hydrophobins form two-dimensional crystals on the air-water interface.[20,21] While much is known about the macroscopic behaviour of these assemblies, less is known about the microscopic structure of these and the initial stages of film formation on liquid interfaces. This is particularly hampered by the lack of data on the structure of these proteins. To date the structures of only three hydrophobins have been determined (using X-ray crystallography[22,23] and NMR[24]). The class-II hydrophobin HFBII, expressed by *Trichoderma Reesei*, has attracted particular attention, due to its high surface activity. X-ray studies show that it is a compact globular protein, with approximate dimensions $30\times27\times24$ Å.[22] The closely related protein HFBI (also a class-II) hydrophobin has also been studied through crystallography,[23] and found to have similar structure and size to HFBII (approximately $30\times26\times25$ Å). The ability to study the initial stages of interfacial aggregation and self-assembly of proteins is also limited. In contrast these are the length and timescales for which molecular simulation is ideally suited. Molecular dynamics and Monte Carlo simulations have already been used to study adsorption of nanoparticles,[25–29] small biosurfactants,[30,31] and proteins[32–34] at liquid interfaces. However, the behaviour of hydrophobins at liquid interfaces has attracted little previous attention by molecular simulations, with only two previous studies of the class-I hydrophobin SC3,[35,36] so there is a clear need for further simulation studies on these proteins.

In this paper molecular dynamics simulations using a chemically-detailed coarse-grain model are used to study the adsorption of the class-II hydrophobins HFBII and HFBI both from *Trichoderma Reesei*), onto the water-octane interface, which may be regarded as an archetypal example of a hydrophilic-hydrophobic interface. In particular the adsorption free energy for these two proteins is determined from the simulations. Due to its status as the exemplar hydrophobin understanding the interfacial behaviour of HFBII is of particular interest. In order to gain insight into the factors that control the interfacial adsorption of HFBII, studies of uniform pseudoproteins are used to determine the effect of the distinctive surface structure and while simulations with the protein held rigid were used to examine the role of protein flexibility on interfacial adsorption.

Model and methodology

Due to the size of systems considered a fully atomistic study is computationally impractical. Instead a coarse-grain model was used, specifically the Shinoda-DeVane-Klein (SDK) model.[37–40] Within this model a single bead typically represents 3-5 heavy atoms (one water bead represents three water molecules). The system consisted of a single hydrophobin (HFBII or HFBI) placed at a water-octane interface, with 8000 water beads (corresponding to 24000 water molecules) initially placed in the region $z < 0$ and 2676 octane molecules in the region $z > 0$. For water and simple fluids this model has been throughly parameterized against thermodynamic properties (densities, interfacial tensions, transfer free energies) and has been applied successfully to study a range of soft matter systems.[41,42] Parameters for amino acids were parameterized against protein crystal structures and water-oil transfer free energies. Intramolecular interactions for octane and proteins were described using the following expressions

$$U_{bond} = k_\ell(\ell - \ell_0)^2 \tag{1a}$$

$$U_{angle} = k_\theta(\theta - \theta_0)^2 + U_{vdw}^{rep}(r) \tag{1b}$$

$$U_{dih} = k_\phi(1 + \cos(m\phi + \delta)), \tag{1c}$$

where k_ℓ, k_θ, and k_ϕ are bond stretching, bond angle bending, and torsional rotation force constants, ℓ_0 and θ_0 are equilibrium bond lengths and angles, and m and δ are the multiplicity and phase angle. In equation 1b $U_{vdw}^{rep}(r)$ is the repulsive part of the van der Waals interaction between the outer atoms in the angle. For octane force field parameters describing bond stretching and bending were taken from Ref,[37] while parameters for proteins were determined using Boltzmann inversion from atomistic molecular dynamics simulations. Disulphide bonds were explicitly described through harmonic bonds between side-chain beads in the cysteine residues. The parameters are listed in the supporting information. In comparision to the commonly used Martini coarse-grained force field[43,44] the SDK model used in this work was parameterized against interfacial properties, such as surface and interfacial tensions and thus provides a more accurate representation of interfacial systems.

The initial structure of the proteins were taken from X-ray crystal structures.[22,23] Each octane molecule consisted of three CG-beads, one $CH_3CH_2CH_2$ (CT in the SDK terminology), one $CH_2CH_2CH_2$ (CM), and one CH_3CH_2 (CT2). The models for HFBII and octane are illustrated in Figure 1.

In order to test the effect of protein flexibility on interfacial adsorption simulations of a rigid model of HFBII are also performed. Two different structures are considered; the first (model A) was a representative structure taken from a simulation of HFBII in bulk water. The second (model B) was taken from the crystal structure from X-ray crystallography.[22] In both cases the protein was considered a rigid body, otherwise the simulation methodology is identical to the flexible case.

Free energy profiles were determined from steered molecular dynamics (SMD) simulations,[45] with the free energy determined from the work using the Jarzynski equality[46]

$$\beta F(z) = -\log\langle \exp\left(-\beta W(z)\right)\rangle \tag{2}$$

where $\beta^{-1} = k_{\mathrm{B}}T$. The guiding potential was a harmonic spring

$$V_{SMD} = \frac{1}{2}k(z_{com}(t) - z_0(t))^2 \tag{3}$$

where $k = 50$ kcal mol^{-1} Å^{-2} and $z_0(t) = z_0(0) + vt$, where $v = 5$ Å ns^{-1} is the pulling velocity. The work profiles determined from simulation are smoothed using a modified weighted histogram method.[47]

In order to localize the interface near the centre of the simulation cell, the system was confined by repulsive Lennard-Jones walls in the *z*-direction (periodic boundaries were applied in the *x* and *y* directions). The equations of motion were integrated using a two-level, multiple-timestep (RESPA) algorithm,[48] with a 2 fs inner timestep (bonded interactions) and a 10 fs outer timestep (van der Waals and electrostatic interactions). The simulations were performed in the NPT ensemble using a Nosé-Hoover thermostat and barostat,[49] with a relaxation time of 1 ps. For all simulations temperature and pressure were set to 303 K and 1 atm. Long range electrostatic interactions were evaluated using a PPPM sum,[50] with a convergence parameter of 0.137 Å^{-1} and 18, 18, and 36 grid points in the *x*, *y*, and *z* directions. Van der Waals interactions were cut-off at 15 Å. All simulations were performed using the LAMMPS simulation package[51]

Results

Interfacial adsorption strength

Shown in Figure 2 are the free energy profiles for the two hydrophobins (HFBII and HFBI) at the water-octane interface. Both HFBII and HFBI are strongly interfacially active, with desorption free energies of the order of 80-120 $k_B T$. Interfacial adsorption is then essentially irreversible which is consistent with the biological functions of these proteins. The desorption free energies are comparable to those found for synthetic nanoparticles, from both molecular simulation[27–29] and experimental measurements.[52] The adsorption strengths are significantly larger than those found for small surfacants and biomolecules. Mukerjee and Handa determined the adsorption free energy for a number of ionic surfactants finding adsorption strengths in the range 6-14 kcal mol^{-1}.[53] Hydrophobins also adsorb more strongly than other biomolecules; recent simulation work on bile salts at an oil-water interface found an adsorption free energies in the range 19-24.9 kcal mol^{-1},[31]

while experimental measurements have found typical adsorption free energies 9.7-22.1 kcal mol^{-1} for bile salts at the air-water interface.[54]

Comparison between the free energy profiles for HFBII and HFBI show that despite the close similarity of these proteins, they have markedly different interfacial adsorption properties. In particular HFBII is hydrophilic (barrier to desorption is lower towards water than towards octane), whereas HFBI is slightly hydrophobic. This difference may reflect differences in their biological function; HFBII is present on the surface of spores[55] whereas HFBI resides in the more hydrophobic cell wall.[56] This is also consistent with the larger hydrophobic patch on HFBI[23] (738-774 $Å^2$ for HFBI compared to 727-740 $Å^2$ for HFBII). This difference in behaviour, however, is not immediately apparent in studies of hydrophobin layers at fluid interfaces, which have found identical structures for HFBII and HFBI.[20] This may be due to the strong association of these proteins in solution and at interfaces which may reduce the influence of the hydrophobic patch. Further studies on the adsorption of hydrophobin dimers and tetramers may be used to provide more insight into this.

The free energy profiles are qualitatively similar to those for nanoparticles; in particular there is no free energy barrier so interfacial adsorption is essentially diffusion-limited. For synthetic nanoparticles experimental[52] and simulation[29] studies have shown free energy barriers to adsorption, under certain circumstances (such as interface deformation, electrostatic interactions, or rearrangement of ligands), which appear to be absent in this case. The range of the interaction between the protein and the interface is larger than protein radius, similar to nanoparticles, which is due to the finite width of the interface caused by interface fluctuations (such as capillary waves[25,57]).

On passing through the water-octane interface there is little change in protein structure. Shown in Figure 3(a) is the average radius of gyration of HFBII and HFBI. In both cases only slight changes in structure are seen, with the difference in R_g between the water and octane phases smaller than the standard deviation of R_g. This shows that the structure of the proteins is essentially unchanged indicating no unfolding of the protein at the interface. This is consistent with experimental studies of HFBII at air-water interface which have shown little change to secondary structure.[58]

As the primary function of these proteins revolves around their interfacial adsorption so it may be expected that the structure of these proteins remains unchanged upon interfacial adsorption.

The shape of the protein can also be approximately characterized by the equivalent inertia spheroid. This is a spheroid with an uniform mass density and the same total mass M as the protein. The dimensions of this give an approximate measure of molecular length, breadth, and width. These are found from the principal moments of inertia I_{xx}, I_{yy}, and I_{zz}, given by the eigenvalues of the inertia tensor

$$I_{\alpha\beta} = \sum_{i=1}^{N_{bead}} m_i (r_i^2 \delta_{\alpha\beta} - r_{i\alpha} r_{i\beta}) \tag{4}$$

where the sum runs over the beads in the protein, m_i is the mass of the ith bead, $\boldsymbol{r}_i$ is the separation vector between the ith bead and the protein centre of mass, and $\delta_{\alpha\beta}$ is the Kronecker delta function. The axis lengths a_λ are then given by[59]

$$a_x = 2\sqrt{\frac{2.5(I_{yy} + I_{zz} - I_{xx})}{M}} \tag{5a}$$

$$a_y = 2\sqrt{\frac{2.5(I_{zz} + I_{xx} - I_{yy})}{M}} \tag{5b}$$

$$a_z = 2\sqrt{\frac{2.5(I_{xx} + I_{yy} - I_{zz})}{M}}. \tag{5c}$$

It is convenient to order these in order to size (a_{max}, a_{mid}, a_{min}). For both HFBII and HFBI these axis lengths have only small differences in the water phase, octane phase, and the interfacial region (Figure 3(b) and (c)). For HFBII a_{max} increases slightly on going into the oil phase, which may be due to rearrangements in amino acid sidechains in the hydrophobic region of the protein, while a_{mid} and a_{min} are approximately constant. In contrast HFBI is shorter in octane than in water, with a_{mid} being slightly larger in octane than in water.

From a macroscopic point of view the adsorption free energy may be estimated from the change in water-octane interfacial area from[60]

$$\Delta F = \gamma_{OW} \Delta A_{OW} \tag{6}$$

where γ_{OW} is the octane-water interfacial tension and ΔA_{OW} is the decrease in water-octane interfacial area, which may be estimated from the axis lengths of the protein. Taking $\gamma_{OW} = 50.74$ mN m^{-1} [61] and estimating $\Delta A_{OW} = \pi a_{max} a_{min}$ gives $\Delta F \approx 36$ kcal mol^{-1}, which is lower than the simulation results. This underestimation may be due to neglect of the protein-solvent interaction, line tensions, and capillary-waves in Eqn 6.

Effect of protein sequence

Due to their nanometre size and relative rigidity it is tempting to regard hydrophobins as analogous to synthetic nanoparticles, in particular to Janus (amphiphilic) particles. It is then an open question how much of the interfacial activity of hydrophobins may be explained in terms of their size and shape (i.e. as 'Pickering' emulsifiers[62]) and how much is due to the protein sequence. In order to shed light on this simulations were performed on pseudo-HFBII proteins with uniform particle types. Specifically three different systems were considered; a uniformly hydrophilic protein, with the interaction between the protein and solvent beads described using van der Waals parameters for EO-type (etheylene oxide) beads, a uniformly hydrophobic protein, with the interactions between the protein and solvent beads described using parameters for CM-type beads, and a uniform protein with the van der Waals ε parameter describing the interaction between the protein and solvent beads given by the average of those for the native protein (given explicitly in Table 1).

Shown in Figure 4 are the free energy profiles for the pseudo-HFBII proteins. As may be expected the uniform hydrophilic and and hydrophobic proteins preferentially reside in the water and oil phases respectively. In both cases, however, a very slight minimum near the interface remains due to the decrease in the water-octane interfacial area (hence interfacial free energy) when the protein is in the vicinity of the interface. Similar weak interfacial adsorption has also been seen in simulations of nanoparticles that are completely wet by one solvent.[26] The barrier for entry into water (octane) phase for the hydrophilic (hydrophobic) proteins are however comparable to a few $k_B T$ suggesting that interfacially-bound proteins may be easily desorbed due to thermal motion.

The uniform average protein is more strongly bound to the interface than the hydrophilic and hydrophobic proteins. However, unlike the native HFBII this is slightly hydrophobic rather than hydrophilic; barrier to entry into the octane phase is substantially lower than for entry into water (23 kcal mol^{-1} rather than 70 kcal mol^{-1}). This hydrophobic character is contrary to the overall hydrophilic character of the native protein and is due to the preponderance of highly hydrophobic residues (valine, leucine, isoleucine). Simulations of single beads using the interaction parameters in Table 1 give an octane-water transfer free energy ~ 0.8 kcal mol^{-1}, confirming the overall hydrophobic nature of the uniform protein and emphasizing the importance of the proteins surface structure to its interfacial behaviour.

Protein flexibility

As the structure of HFBII is relatively unchanged on going through the water-octane interface it may be expected that protein flexibility would have little effect on the interfacial adsorption of HFBII. Shown in Figure 5 are the free energy profiles for these rigid proteins. For model A the free energy profile is largely similar to the flexibile protein, although the barrier for energy into the bulk water region is higher, suggesting that protein flexibility plays a role in stabilising the protein in water (potentially due to entropic effects). For model B (structure taken from crystallography) is significantly different to the flexible protein; specifically the free energy barrier for entry into the octane region is now lower than for entry into water (the protein is now overall hydrophobic). This hydrophobic behaviour may be understood as the crystal is largely devoid of water hence hydrophobic residues are more likely to be exposed to the outside, which is likely to be enhanced by the strong dimerisation of these proteins in the crystal, with the hydrophobic patches on neighbouring proteins in contact.

Conclusions

Using coarse-grained molecular dynamics simulations the adsorption of hydrophobins, small, amphiphilic proteins, at the water-octane interface has been studied. Two typical examples, HFBII and HFBI, have been studied. In both cases these are strongly interfacially active, with desorption barriers typically 80-120 $k_{\mathrm{B}}T$, indicating essentially irreversible adsorption on the interface. This adsorption free energy is comparable to values for synthetic nanoparticles and significantly larger than small molecule surfactants and biomolecules. The protein-interface interaction is also similar to that seen from recent simulation studies of synthetic nanoparticles at liquid interfaces - in particular the interaction range is larger than the protein size and there is no appreciable barrier to adsorption, suggesting that the initial stages of film formation are diffusion limited. Only small changes in protein structure are seen between the bulk water, bulk octane, and interfacial regions.

The simulations were also used to assess some of the factors that affect interfacial adsorption. The distinctive surface structure of these proteins is expected to play a key role in their interfacial adsorption, which is born out by the behaviour of uniform analogues. In particular uniformly hydrophobic and hydrophilic proteins are found to preferentially reside in oil and water phases respectively. When the interactions between the protein and solvent beads are replaced by the averaged values the protein remains surface active but becomes less hydrophobic rather than hydrophilic. This is due to the preponderance of highly hydrophobic amino acids; from simulation of a single averaged bead the octane-water transfer free energy is ~ 0.8 kcal mol^{-1} (i.e. is hydrophobic), confirming the overall hydrophobic behaviour in this case. Protein flexibility also has an effect of the interfacial adsorption of HFBII, in particular neglecting flexibility makes the protein less hydrophilic.

In order to make the molecular dynamics simulations computationally efficient a realistic coarse-grain model was employed, which has been thoroughly validated against thermodynamic properties, such as interfacial tensions or transfer free energies. Thus it may be expected to accurately reproduce properties such as adsorption free energies calculated here. Due to its lower resolution, however, it may not reproduce fine structural information. Recent comparison between

all-atom and coarse-grain simulations (using the Martini model) have shown that coarse-grain models may underestimate penetration of proteins into hydrophobic liquids,[34] although this is likely to be model dependent and further investigation, such as comparision between atomistic and CG models would be required.

While the aim of this study has been to study the adsorption of hydrophobins at the oil-water interface, which has particular relevance to their materials applications, HFBII and HFBI are also known to interaction strongly with lipid bilayers.[56] In many previous studies the oil-water interface has been used as a simple model of a lipid membrane and the present results suggest that HFBII and HFBI would also adsorb strongly onto these. It should, however, be cautioned that due to the highly ordered lipid head groups and (depending on the phase) tail groups would provide a significant entropic barrier to adsorption. As lipid molecules, along with both ionic and non-ionic surfactants, have been parameterised in the SDK force field,[63] this would potentially form an interesting avenue for further work.

Acknowledgements

The author is grateful to Russell DeVane for providing CG-protein force field parameters ahead of publication and Phillip Cox for helpful conversations. Computer resources for this work were provided by the Centre for Scientific Computing, University of Warwick and this work was funded by the Leverhulme Trust (ECF/2010/0254).

Supporting information available

Details of force field and force field parameters. This information is available free of charge via the Internet at http://pubs.acs.org/.

References

(1) Lu, J. R.; Zhao, X.; Yaseen, M. Biomimetic amphiphiles: Biosurfactants. *Curr. Opin. Coll. Inter. Sci.* **2007**, *12*, 60–67.

(2) Cooper, A.; Kennedy, M. W. Biofoams and natural protein surfactants. *Biophys. Chem.* **2010**, *151*, 96–104.

(3) Reis, P.; Holmberg, K.; Watzke, H.; Leser, M. E.; Miller, R. Lipases at interfaces: a review. *Adv. Coll. Inter. Sci.* **2008**, *147-148*, 237–50.

(4) Head, J. F.; Mealy, T. R.; McCormack, F. X.; Seaton, B. A. Crystal structure of trimeric carbohydrate recognition and neck domains of surfactant protein A. *J. Bio. Chem.* **2003**, *278*, 43254–60.

(5) Wierenga, P.; Gruppen, H. New views on foams from protein solutions. *Curr. Opin. Coll. Inter. Sci.* **2010**, *15*, 365–373.

(6) Kokkonen, H. E.; Ilvesaro, J. M.; Morra, M.; Schols, H. A.; Tuukkanen, J. Effect of modified pectin molecules on the growth of bone cells. *Biomacromolecules* **2007**, *8*, 509–15.

(7) Fairman, R.; Akerfeldt, K. S. Peptides as novel smart materials. *Curr. Opin. Struct. Bio.* **2005**, *15*, 453–63.

(8) Livney, Y. D. Milk proteins as vehicles for bioactives. *Curr. Opin. Coll. Inter. Sci.* **2010**, *15*, 73–83.

(9) Linder, M. B. Hydrophobins: Proteins that self assemble at interfaces. *Curr. Opin. Coll. Inter. Sci.* **2009**, *14*, 356–363.

(10) Wessels, J. G. H. Developmental Regulation of Fungal Cell Wall Formation. *Ann. Rev. Phytopath.* **1994**, *32*, 413–437.

(11) Wessels, J. G. H.; De Vries, O. M. H.; Asgeirsdottir, S.; Springer, J. The thn mutation of Schizophyllum commune, which suppresses formation of aerial hyphae, affects expression of the Sc3 hydrophobin gene. *J. Gen. Micro.* **1991**, *137*, 2439–2445.

(12) van Wetter, M.-A.; Wosten, H. A. B.; Wessels, J. G. H. SC3 and SC4 hydrophobins have distinct roles in formation of aerial structures in dikaryons of Schizophyllum commune. *Mol. Microbio.* **2000**, *36*, 201–210.

(13) Cox, A. R.; Aldred, D. L.; Russell, A. B. Exceptional stability of food foams using class II hydrophobin HFBII. *Food Hydrocoll.* **2009**, *23*, 366–376.

(14) Tchuenbou-Magaia, F.; Norton, I.; Cox, P. Hydrophobins stabilised air-filled emulsions for the food industry. *Food Hydrocoll.* **2009**, *23*, 1877–1885.

(15) Lumsdon, S. O.; Green, J.; Stieglitz, B. Adsorption of hydrophobin proteins at hydrophobic and hydrophilic interfaces. *Coll. Surf. B* **2005**, *44*, 172–8.

(16) Janssen, M.; van Leeuwen, M.; Scholtmeijer, K.; van Kooten, T.; Dijkhuizen, L.; Wösten, H. Coating with genetic engineered hydrophobin promotes growth of fibroblasts on a hydrophobic solid. *Biomaterials* **2002**, *23*, 4847–4854.

(17) Valo, H. K.; Laaksonen, P. H.; Peltonen, L. J.; Linder, M. B.; Hirvonen, J. T.; Laaksonen, T. J. Multifunctional hydrophobin: toward functional coatings for drug nanoparticles. *ACS Nano* **2010**, *4*, 1750–8.

(18) Laaksonen, P.; Walther, A.; Malho, J.-M.; Kainlauri, M.; Ikkala, O.; Linder, M. B. Genetic Engineering of Biomimetic Nanocomposites: Diblock Proteins, Graphene, and Nanofibrillated Cellulose. *Angew. Chem. Int. Ed.* **2011**, *50*, 8688–8691.

(19) Devocht, M.; Scholtmeijer, K.; van der Vegte, E.; de Vries, O.; Sonveaux, N.; Wosten, H.; Ruyschaert, J.; Hadziionnou, G.; Wessels, J.; Robillard, G. Structural Characterization of

the Hydrophobin SC3, as a Monomer and after Self-Assembly at Hydrophobic/Hydrophilic Interfaces. *Biophys. J.* **1998**, *74*, 2059–2068.

(20) Kisko, K.; Szilvay, G. R.; Vuorimaa, E.; Lemmetyinen, H.; Linder, M. B.; Torkkeli, M.; Serimaa, R. Self-assembled films of hydrophobin proteins HFBI and HFBII studied in situ at the air/water interface. *Langmuir* **2009**, *25*, 1612–9.

(21) Zhang, X. L.; Penfold, J.; Thomas, R. K.; Tucker, I. M.; Petkov, J. T.; Bent, J.; Cox, A.; Campbell, R. a. Adsorption behavior of hydrophobin and hydrophobin/surfactant mixtures at the air-water interface. *Langmuir* **2011**, *27*, 11316–23.

(22) Hakanpää, J.; Paananen, A.; Askolin, S.; Nakari-Setälä, T.; Parkkinen, T.; Penttilä, M.; Linder, M. B.; Rouvinen, J. Atomic resolution structure of the HFBII hydrophobin, a self-assembling amphiphile. *J. Bio. Chem.* **2004**, *279*, 534–9.

(23) Hakanpää, J.; Szilvay, G. R.; Kaljunen, H.; Maksimainen, M.; Linder, M.; Rouvinen, J. Two crystal structures of Trichoderma reesei hydrophobin HFBI–the structure of a protein amphiphile with and without detergent interaction. *Protein Sci* **2006**, *15*, 2129–40.

(24) Kwan, A. H.; Macindoe, I.; Vukasin, P. V.; Morris, V. K.; Kass, I.; Gupte, R.; Mark, A. E.; Templeton, M. D.; Mackay, J. P.; Sunde, M. The Cys3-Cys4 loop of the hydrophobin EAS is not required for rodlet formation and surface activity. *J. Mol. Bio.* **2008**, *382*, 708–20.

(25) Cheung, D. L.; Bon, S. A. F. Interaction of Nanoparticles with Ideal Liquid-Liquid Interfaces. *Phys. Rev. Lett.* **2009**, *102*, 066103/1–4.

(26) Cheung, D. L.; Bon, S. A. F. Stability of Janus nanoparticles at fluid interfaces. *Soft Matter* **2009**, *5*, 3969.

(27) Udayana Ranatunga, R. J. K.; Kalescky, R. J. B.; Chiu, C.-C.; Nielsen, S. O. Molecular Dynamics Simulations of Surfactant Functionalized Nanoparticles in the Vicinity of an Oil/Water Interface. *J. Phys. Chem. C* **2010**, *114*, 12151–12157.

(28) Fan, H.; Resasco, D. E.; Striolo, A. Amphiphilic silica nanoparticles at the decane-water interface: insights from atomistic simulations. *Langmuir* **2011**, *27*, 5264–74.

(29) Cheung, D. L. Molecular dynamics study of nanoparticle stability at liquid interfaces: effect of nanoparticle-solvent interaction and capillary waves. *J. Chem. Phys.* **2011**, *135*, 054704.

(30) Gang, H.-Z.; Liu, J.-F.; Mu, B.-Z. Interfacial behavior of surfactin at the decane/water interface: a molecular dynamics simulation. *J. Phys. Chem. B* **2010**, *114*, 14947–54.

(31) Euston, S. R.; Bellstedt, U.; Schillbach, K.; Hughes, P. S. The adsorption and competitive adsorption of bile salts and whey protein at the oilâĂŞwater interface. *Soft Matter* **2011**, *7*, 8942.

(32) Euston, S. R.; Hughes, P.; Naser, M. A.; Westacott, R. E. Comparison of the adsorbed conformation of barley lipid transfer protein at the decane-water and vacuum-water interface: a molecular dynamics simulation. *Biomacromolecules* **2008**, *9*, 1443–53.

(33) Euston, S. R.; Hughes, P.; Naser, M. A.; Westacott, R. E. Molecular dynamics simulation of the cooperative adsorption of barley lipid transfer protein and cis-isocohumulone at the vacuum-water interface. *Biomacromolecules* **2008**, *9*, 3024–32.

(34) Euston, S. R. Molecular dynamics simulation of protein adsorption at fluid interfaces: a comparison of all-atom and coarse-grained models. *Biomacromolecules* **2010**, *11*, 2781–7.

(35) Zangi, R.; de Vocht, M. L.; Robillard, G. T.; Mark, A. E. Molecular dynamics study of the folding of hydrophobin SC3 at a hydrophilic/hydrophobic interface. *Biophys. J.* **2002**, *83*, 112–24.

(36) Fan, H.; Wang, X.; Zhu, J.; Robillard, G. T.; Mark, A. E. Molecular dynamics simulations of the hydrophobin SC3 at a hydrophobic/hydrophilic interface. *Proteins* **2006**, *64*, 863–73.

(37) Shinoda, W.; DeVane, R.; Klein, M. L. Multi-property fitting and parameterization of a coarse grained model for aqueous surfactants. *Mol. Sim.* **2007**, *33*, 27–36.

(38) DeVane, R.; Shinoda, W.; Moore, P. B.; Klein, M. L. Transferable Coarse Grain Nonbonded Interaction Model for Amino Acids. *J. Chem. Theory Comput.* **2009**, *5*, 2115–2124.

(39) Chiu, C.-C.; DeVane, R.; Klein, M. L.; Shinoda, W.; Moore, P. B.; Nielsen, S. O. Coarse-grained potential models for phenyl-based molecules: I. Parametrization using experimental data. *J. Phys. Chem. B* **2010**, *114*, 6386–93.

(40) DeVane, R. H. personal communication.

(41) Shinoda, W.; DeVane, R.; Klein, M. L. Coarse-grained molecular modeling of non-ionic surfactant self-assembly. *Soft Matter* **2008**, *4*, 2454.

(42) Khurana, E.; DeVane, R. H.; Kohlmeyer, A.; Klein, M. L. Probing peptide nanotube self-assembly at a liquid-liquid interface with coarse-grained molecular dynamics. *Nano Lett.* **2008**, *8*, 3626–30.

(43) Marrink, S. J.; Risselada, H. J.; Yefimov, S.; Tieleman, D. P.; de Vries, A. H. The MARTINI force field: coarse grained model for biomolecular simulations. *J. Phys. Chem. B* **2007**, *111*, 7812–24.

(44) Monticelli, L.; Kandasamy, S. K.; Periole, X.; Larson, R. G.; Tieleman, D. P.; Marrink, S.-j. The MARTINI Coarse-Grained Force Field : Extension to Proteins. *J. Chem. Theory Comp.* **2008**, *4*, 819–834.

(45) Park, S.; Schulten, K. Calculating potentials of mean force from steered molecular dynamics simulations. *J. Chem. Phys.* **2004**, *120*, 5946–61.

(46) Jarzynski, C. Nonequilibrium Equality for Free Energy Differences. *Phys. Rev. Lett.* **1997**, *78*, 2690–2693.

(47) Cuendet, M. A.; Michielin, O. Protein-protein interaction investigated by steered molecular dynamics: the TCR-pMHC complex. *Biophys. J.* **2008**, *95*, 3575–90.

(48) Tuckerman, M.; Berne, B. J.; Martyna, G. J. Reversible multiple time scale molecular dynamics. *J. Chem. Phys.* **1992**, *97*, 1990.

(49) Martyna, G. J.; Tobias, D. J.; Klein, M. L. Constant pressure molecular dynamics algorithms. *J. Chem. Phys.* **1994**, *101*, 4177.

(50) Hockney, R. W.; Eastwood, J. W. *Computer simulations using particles*; Adam Hilger: Bristol, 1988.

(51) Plimpton, S. J. Fast Parallel Algorithms for Short-Range Molecular Dynamics. *J. Comp. Phys.* **1995**, *117*, 1–19.

(52) Du, K.; Glogowski, E.; Emrick, T.; Russell, T. P.; Dinsmore, A. D. Adsorption Energy of Nano- and Microparticles at Liquid-Liquid Interfaces. *Langmuir* **2010**, *26*, 12518–12522.

(53) Mukerjee, P.; Handa, T. Adsorption of fluorocarbon and hydrocarbon surfactants to air-water, hexane-water and perfluorohexane-water interfaces. Relative affinities and fluorocarbon-hydrocarbon nonideality effects. *J. Phys. Chem.* **1981**, *85*, 2298–2303.

(54) Jana, P. K.; Moulik, S. P. Interaction of bile salts with hexadecyltrimethylammonium bromide and sodium dodecyl sulfate. *J. Phys. Chem.* **1991**, *95*, 9525–9532.

(55) Nakari-Setala, T.; Aro, N.; Ilmén, M.; Munoz, G.; Kalkkinen, N.; Penttila, M. Differential Expression of the Vegetative and Spore-Bound Hydrophobins of Trichoderma Reesei Cloning and Characterization of the Hfb2 Gene. *Eur. J. Biochem.* **1997**, *248*, 415–423.

(56) Nakari-Setala, T.; Aro, N.; Kalkkinen, N.; Alatalo, E.; Penttila, M. Genetic and Biochemical Characterization of the Trichoderma Reesei Hydrophobin HFBI. *Eur. J. Biochem.* **1996**, *235*, 248–255.

(57) Lehle, H.; Oettel, M. Stability and interactions of nanocolloids at fluid interfaces: effects of capillary waves and line tensions. *J. Phys. Condens. Matt.* **2008**, *20*, 404224/1–11.

(58) Askolin, S.; Linder, M.; Scholtmeijer, K.; Tenkanen, M.; Penttilä, M.; de Vocht, M. L.; Wösten, H. A. B. Interaction and comparison of a class I hydrophobin from Schizophyllum commune and class II hydrophobins from Trichoderma reesei. *Biomacromolecules* **2006**, *7*, 1295–301.

(59) Müller, J. J.; Schrauber, H. The inertia-equivalent ellipsoid: a link between atomic structure and low-resolution models of small globular proteins determined by small-angle X-ray scattering. *J. Appl. Crystallo.* **1992**, *25*, 181–191.

(60) Pieranski, P. Two-dimensional interfacial colloidal crystals. *Phys. Rev. Lett.* **1980**, *45*, 569–572.

(61) Zeppieri, S.; Rodríguez, J.; López de Ramos, A. L. Interfacial Tension of Alkane + Water Systems. *J. Chem Eng. Data* **2001**, *46*, 1086–1088.

(62) Binks, B. P. Particles as surfactants - similarities and differences. *Curr. Opin. Coll. Inter. Sci.* **2002**, *7*, 21–41.

(63) Shinoda, W.; DeVane, R.; Klein, M. L. Zwitterionic lipid assemblies: molecular dynamics studies of monolayers, bilayers, and vesicles using a new coarse grain force field. *J. Phys. Chem. B* **2010**, *114*, 6836–49.

Table 1: Protein-solvent interaction parameters for averaged uniform protein bead. For interaction types LJ12-4 and LJ9-6 the pair interactions are given by $U_{LJ12-4}(r) = (3\sqrt{3}/2)\varepsilon((\sigma/r)^{12} - (\sigma/r)^4)$ and $U_{LJ9-6}(r) = (27/4)\varepsilon((\sigma/r)^9 - (\sigma/r)^6)$.

Bead-types	Interaction type	ε / kcal mol^{-1}
U-W	LJ12-4	0.732
U-CT	LJ9-6	0.586
U-CM	LJ9-6	0.555
U-CT2	LJ9-6	0.478

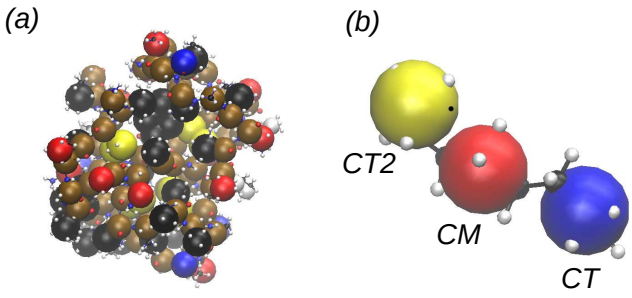

Figure 1: (a) Superposition of atomistic and coarse-grain models of (a) HFBII and (b) octane.

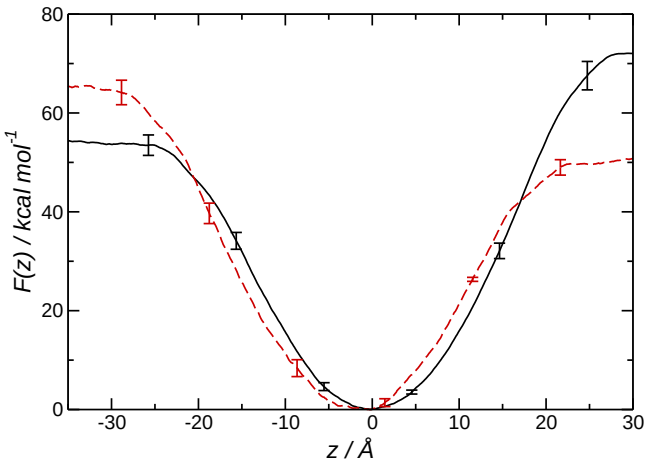

Figure 2: Free energy profiles for HFBII (solid line, black) and HFBI (dashed line, red) at water-octane interface.

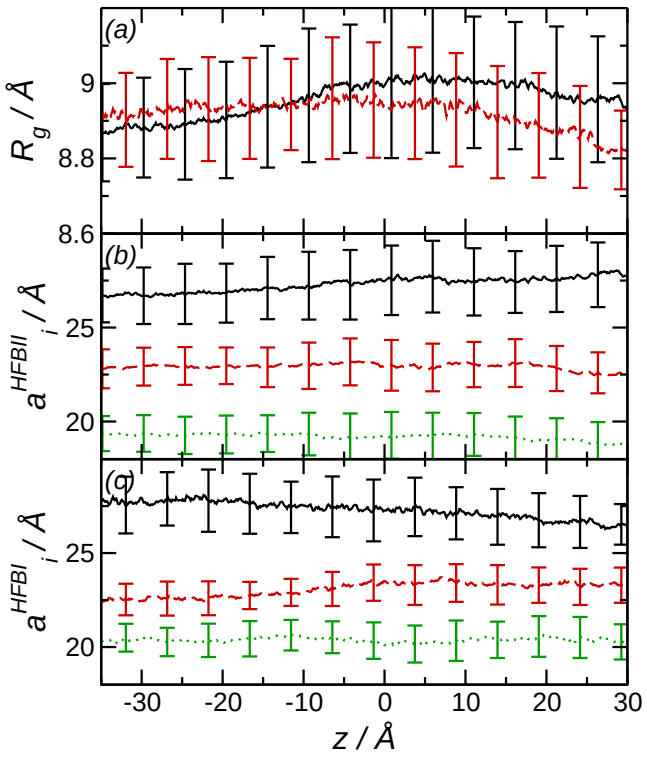

Figure 3: (a) Radius of gyration against protein-interface separation for HFBII (solid line, black) and HFBI (dashed line, red). (b) Axis lengths for the equivalent inertia spheroid against z for HFBII. a_{max}, a_{mid}, and a_{min} denoted by solid line (black), dashed line (red), and dotted line (green). (c) Axis lengths for the equivalent inertia spheroid against z for HFBI. Symbols at in (b).

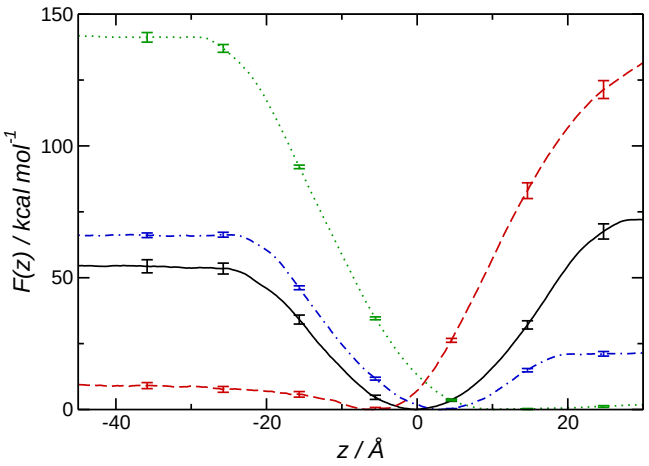

Figure 4: Free energy profiles for native HFBII (solid line, black), hydrophilic HFBII (dashed line, red), hydrophobic HFBII (dotted line, green), and averaged HFBII (dot-dashed line, blue) at water-octane interface.

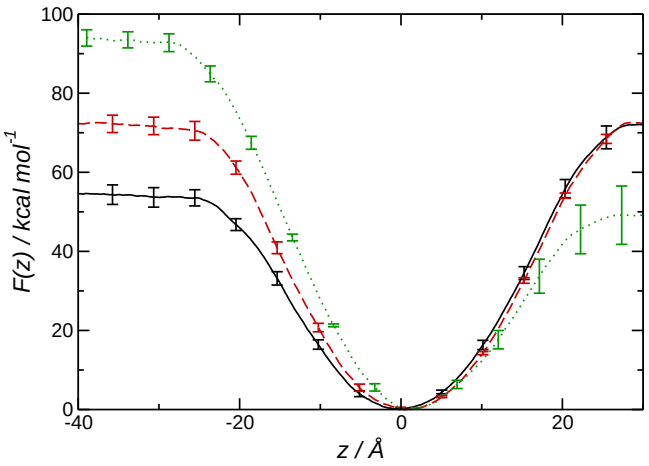

Figure 5: Free energy profile for flexible HFBII (solid line, black), rigid HFBII (dashed line, red), and rigid HFBII using X-structure (dotted line, green).

Table of contents only